

# A Sustainable Approach for the Development of Cellulose-Based Food Container from Coconut Coir

Md. Hafizul Islam, Mosummath Hosna Ara,\* Mubarak A. Khan, Jannatul Naime, Md. Latifur Rahman, Tania Akter Ruhane, and Md. Abu Rayhan Khan



Cite This: *ACS Omega* 2025, 10, 157–169



Read Online

ACCESS |



Metrics & More



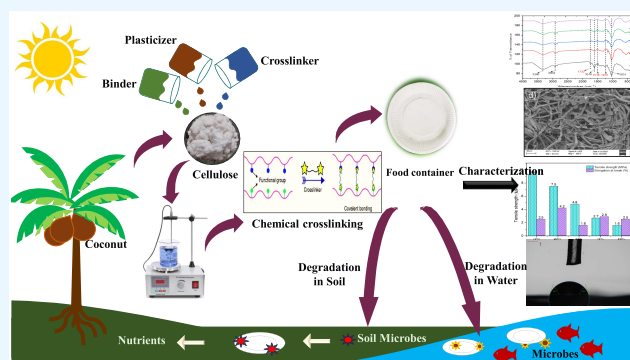
Article Recommendations



Supporting Information

**ABSTRACT:** The increasing demand for sustainable resources has revived the research on cellulose over the last decades. Therefore, the current research focused on the synthesis of biopolymers for the development of viable tableware utensils from cellulose of coconut coir. The synthesized biopolymer was characterized by using Fourier transform infrared (FT-IR) spectroscopy, thermogravimetric analysis (TGA), scanning electron microscopy (SEM), X-ray diffraction (XRD), tensile strength, and contact angle. The synthesized biopolymer was converted to workable conditions through incorporation of starch, as a binder, at various ratios with cellulose, ranging from 1:9 to 10:0. Moreover, the most prominent features of the synthesized biopolymer were obtained by the addition of glycerin as a plasticizer and citric acid as a cross-linker.

At 6:4 ratio of cellulose and binder showed excellent mechanical properties, and with the incorporation of cross-linker, the biopolymer possessed high tensile strength (18.6 MPa) and elongation (3.5%) in comparison to commercially available polystyrene polymer (1.5 MPa) and (2.6%), respectively. Furthermore, the cross-linker citric acid bestows with network structure that was confirmed with the change of contact angle ( $81^\circ$ ), FT-IR spectra, surface morphology, crystallinity index, and water vapor transmission rate ( $573 \text{ g/m}^2/\text{d}$ ). TGA data revealed the improved thermal properties of the biopolymer, and the decomposed temperature was elevated from  $>223$  to  $238^\circ\text{C}$  in the presence of network structure proved by cross-linker. The degree of deterioration was assessed by soil burial test, highlighting the environmental compatibility of the tableware. The purpose of the study was to synthesize sustainable tableware from waste source coir fiber for the reduction of harmful effects of synthetic counterpart.



## 1. INTRODUCTION

Food safety has become a burning question throughout the globe for maintaining the quality and ameliorating the hygiene of the food.<sup>1</sup> In this regard, food containers and tableware may certainly ensure food safety from all kinds of rotten and spoilage by exposure to air, moisture, bacteria, and other contaminants.<sup>2</sup> Conventional food containers made from polystyrene (PS), known as styrofoam, are extensively used all over the world for protection of food. A statistics from 2016 divulged that the use of polystyrene globally increased by approximately 14.7 million metric tons (MMT) per year.<sup>3</sup> The most negative feature of the traditional packaging materials is the vitiation of food that exert detrimental effects on human health.<sup>4</sup> Apart from this, severe environmental pollution has arisen through the widespread usage of nonbiodegradable plastic tableware. Burning of such nonbiodegradable plastic, for instance, elevates the level of toxic gases, including carbon dioxide in the environment, resulting in global warming.<sup>5</sup> It is exigency to develop an alternative source of nondegradable plastic, and environment benign as well as biobased materials may be a suitable solution for the food safety.<sup>5,6</sup>

Recently, researchers have been accentuating biobased packaging materials compared to traditional plastic polymers considering environmental issues as well as food safety.<sup>7</sup> Numerous consumer products have been made from biopolymers such as cellulose, starch, polycaprolactone, polylactic acid (PLA), polybutylene adipate-co-terephthalate (PBAT), etc. Among the biobased polymers, cellulose is the most prevalent natural polymer on earth, and still is gaining attention owing to biodegradability, biocompatibility, renewability, heat stability, availability, high mechanical strength, nontoxicity, and low cost.<sup>8,9</sup> Actually, cellulose is a linear homopolymer of  $\beta$ -D-glucose monomers covalently bonded together by 1–4 glycosidic bonds.<sup>10–12</sup> The significant characteristic of cellulose fiber is the ability to provide

**Received:** March 29, 2024  
**Revised:** October 7, 2024  
**Accepted:** October 8, 2024  
**Published:** December 24, 2024



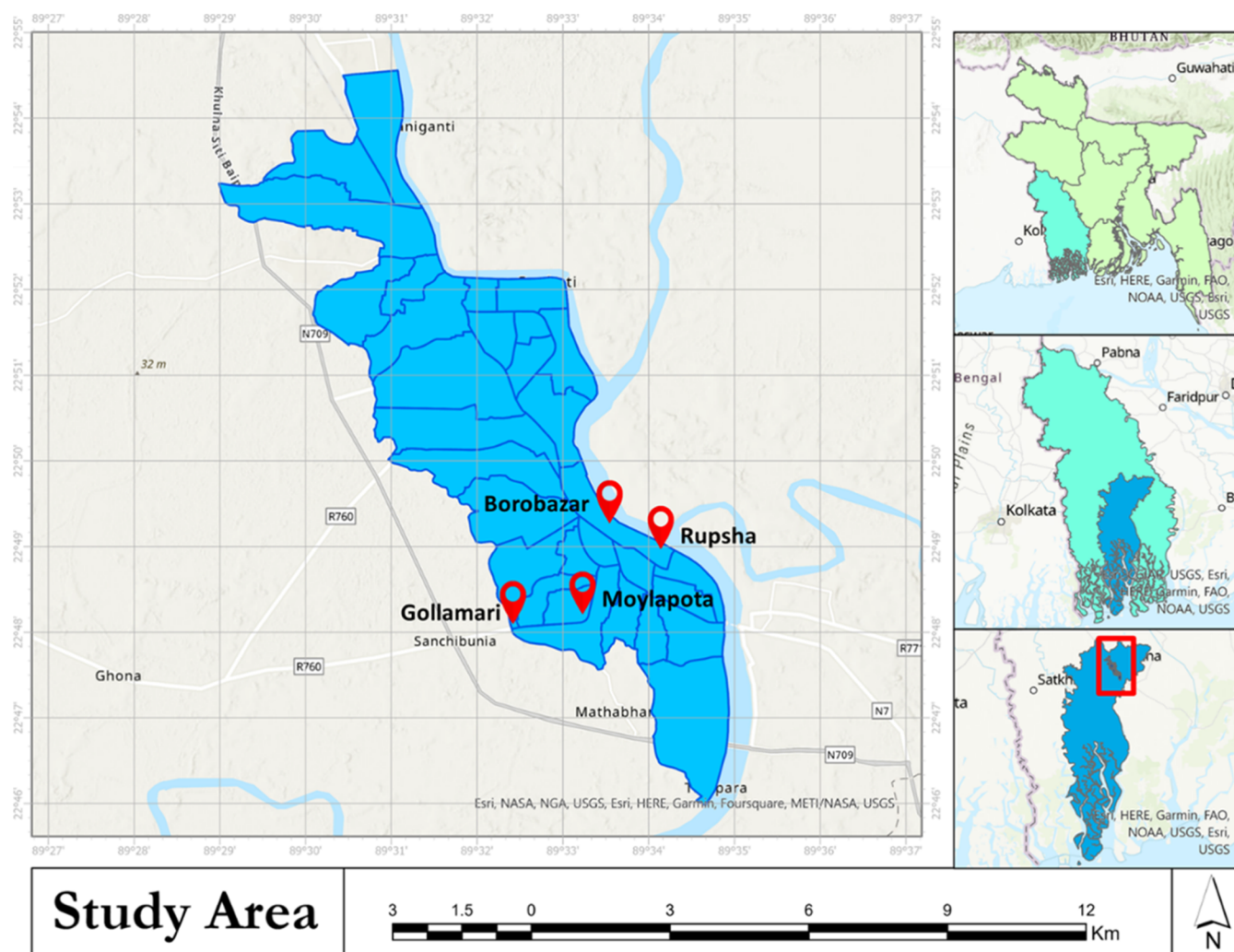


**Figure 1.** Sampling area of coconut coir (Khulna, Bangladesh).

reinforcement to the composite matrix, resulting in the enhancement of mechanical properties, including tensile strength, modulus of elasticity, and impact resistance.<sup>13,14</sup> It can also improve the dimensional stability of composite materials by providing uniformity and structural integrity to the composite.<sup>15</sup> In a study, Mamani et al. reported that cellulose can be used as a reinforcement agent in polymeric matrices with hydrophilic groups, such as starch, poly (ethylene oxide), or poly (vinyl alcohol), and lower processing temperatures are required compared to manufacturing of polyethylene-based utensils.<sup>16</sup>

The present research has focused on the preparation of tableware from coconut coir fiber. The major source of cellulose is derived from plants or plant-based materials. Coconut is a major source of cellulose in tropical Asian countries such as Indonesia, India, Bangladesh, Sri Lanka, and Vietnam. A report of 2018–2019 expressed that the worldwide production of coconuts was 63 million metric tons.<sup>17</sup> Bangladesh has about 2800 ha of coconut land with an average annual coconut production of 431,596 MT and holds 12th position in world coconut production.<sup>18</sup> Coconut fiber, known as coir fiber, is a natural cellulosic fiber found in hard, inner shell and outer layer of coconut.<sup>19</sup> Numerous researches have been conducted on the chemical compositions of coir fiber, and higher percentages of cellulose (32–50%), as well as

other constituents, such as 30–46% lignin, 0.15–2.5% hemicellulose, and around 3–4% pectin, were found.<sup>20,21</sup> Coir fiber has low economic value and most often, it is dumped, burned, or used as organic fertilizer in farmlands.<sup>16</sup> Consequently, coconut coir may be an alternative source of cellulose for the preparation of biopolymer-based products.

The tableware prepared from natural polymers, such as cellulose, is stiff and brittle in nature. Its flexibility and elongation properties can be enhanced through the incorporation of plasticizer into the polymer matrices, indicating the lowering of tensile strength of matrix.<sup>22</sup> Common plasticizers are oligosaccharides, polyols, and lipids, including saturated fatty acids, monoglycerides, ester derivatives, and phospholipids.<sup>23</sup> Of them, glycerol is extensively utilized for the development of packaging materials because of its low cost and high availability.<sup>24</sup> Moreover, biopolymers used in various purports need more mechanical strength that can be achieved through cross-linking. Basically, cross-linking is the process of forming chemical bonds between polymeric chains by the cross-linking agents, such as citric acid, boric acid, and glutaraldehyde, that provides the network structure with the change of physical and chemical properties.<sup>25</sup> In this study, citric acid (CA) was used as a cross-linking agent owing to its availability in various fruits, low cost, and containing one monohydroxy and three carboxyl groups. However, the

presence of multicarboxylic in CA makes esterification possible between CA and the hydroxyl groups of cellulose. Additionally, the multicarboxylic structure creates more hydrogen bonds, enhancing network structure, water resistance, and mechanical strength.<sup>26</sup>

The purpose of this research was to extract cellulose from waste coir fiber and develop environmentally friendly tableware, food container including plate, cup, and box. A novel experimental design was developed for the preparation of tableware. The study also explored the use of glycerol as a plasticizer and CA as a cross-linking agent of different ratios to optimize the preparation of tableware. Throughout the research, environmental deflation can be reduced through the introduction of eco-friendly biopolymer, and the waste product of coconut can be utilized as a value-added product. Moreover, a variety of advanced characterization techniques were used in this research to characterize the chemical structure, thermal stability, surface morphology, hydrophobic property, tensile strength, water vapor permeability, and soil burial tests of the prepared tableware.

## 2. MATERIALS AND METHODS

**2.1. Materials and Chemicals.** The reagents and chemicals used in this study were of analytical grade, and chemicals, including sodium hydroxide (reagent grade, purity  $\geq 98\%$ , pellets- anhydrous), sodium chlorite (technical grade, purity 80%), potato starch (white power), acetic acid (ACS reagent, purity  $\geq 99.7\%$ ), citric acid (ACS reagent, purity  $\geq 99.5\%$ ), and glycerol (ACS reagent, purity  $\geq 99.5\%$ ), were purchased from Sigma-Aldrich for cellulose extraction and preparation of tableware utensils.

**2.2. Sample Collection and Preparation.** Coconuts of *Cocos nucifera* species were collected from Gollamari, Moylapota, Rupsa, and Borobazar, local markets of Khulna (Latitude: 22° 47' 59" N; Longitude: 89° 32' 15" E), Bangladesh, in 2024 (Figure 1). The samples were transported to a laboratory for chopping, sun drying, and cutting into small pieces (approximately 3–5 mm long) and then stored in a container at room temperature for further investigations, including ash, moisture, and cellulose content. The physiological parameters of coconut are given in Table 1.

**Table 1. Physiological Parameters of Coconut**

name of parameters	amount/dimension
weight (g)	1180.48 $\pm$ 38.50
length (mm)	272.59 $\pm$ 7.10
diameter (mm)	178.45 $\pm$ 4.87
perimeter (mm)	680.65 $\pm$ 9.34

**2.2.1. Moisture and Ash Content.** Coconut coir was dried in an electric oven (DSO-500D, Digisystem, Taiwan) at 105 °C for 24 h until a constant weight was obtained, and the moisture content was calculated from the difference between fresh and dry sample weight (eq 1).<sup>27</sup> Another important parameter such as ash was estimated by the ignition of sample at 600 °C for 6 h in a muffle furnace (FTME-705, Korea) (eq 2).<sup>28</sup>

$$\text{moisture (\%)} = \frac{(\text{weight of sample} - \text{weight of dry sample})}{\text{weight of sample}} \times 100\% \quad (1)$$

$$\text{ash (\%)} = \frac{\text{weight of ash}}{\text{weight of sample}} \times 100\% \quad (2)$$

**2.2.2. Cellulose Extraction from Coconut Coir.** For the extraction of cellulose from coconut coir, alkali treatment is necessary to remove the lignin, hemicellulose, pectin, and wax. Compared to cellulose, lignin is more soluble in an alkaline condition.<sup>29</sup> Lignin content of coir fiber reduced by high-temperature NaOH treatment.<sup>16</sup> Previous research has indicated that the brown color of coir is caused owing to the presence of lignin, hemicellulose, and other components. After alkali treatment and bleaching, the fiber becomes white (or light cream).<sup>30,31</sup> In this research, cellulose was extracted from coir fiber using alkali treatment and bleaching process according to a previous method with slight modification.<sup>32</sup> This chemical treatment method was optimized for the extraction of high cellulose content within a short period of time, and utilization of lower energy consumption compared to previous reports.<sup>32–34</sup> Firstly, coconut coir was dried at 60 °C for 4 h to remove excess moisture. A total of 10.0 g of coir was treated with 200 mL of 5, 10, 15, and 20% (w/v) aqueous solution of sodium hydroxide for 4 h at 90 °C under constant mechanical stirring (200 rpm). The alkali-treated fiber was washed with deionized water several times until the alkali was completely removed and turned into neutral. After the bleaching process, pulps were reacted with 300 mL of 2% (w/v) sodium chlorite solution. Then, glacial acetic acid was added to maintain the pH of the solution at 4. The mixture was then stirred at 80 °C for 3 h, and it was washed with deionized water until the pH became neutral. Finally, cellulose was oven-dried (DSO-500D, Digisystem, Taiwan) at 60 °C, and the yield of cellulose from the sample was calculated according to eq 3.

$$\text{cellulose (\%)} = \frac{\text{weight of cellulose}}{\text{weight of sample}} \times 100\% \quad (3)$$

**2.3. Preparation of Tableware Utensils from Coconut Coir.** For the preparation of tableware, cellulose was incorporated with starch as the binder at various ratios, ranging from 10:0 to 1:9 (Step 1). Then, 10–50% (w/w) of glycerin as a plasticizer was added to the overall solute weight of cellulose and starch (Step 2). Finally, 10–50% (w/w) of CA as a chemical cross-linking agent was added to the overall solute weight of cellulose and starch (Step 3), as shown in Table 2. Then, the mixture of compounds was stirred (200 rpm) for 15 min at 80 °C by adding a small amount of distilled water. After each step, samples were taken in a Heat Press Machine (CARVER, Inc. Auto Series Plus, Model: 4533.4PL1000) maintaining given parameters, such as pressure: 5 tones, temperature: 80 °C, time duration: 30 s, and tensile strength and elongation at break were measured by Universal Testing Machine. Finally, by using different molds in heat press machine, tableware utensils, for instance, plate, cup, and box, were fabricated (Figure 2). The optimized ratio of cellulose to starch (w/w) was found at 6:4 with 20% of glycerol and 10% of CA. The tableware was prepared based on their mechanical strengths.

Table 2. Experimental Design of Cellulose-Based Tableware

1 <sup>st</sup> Step	2 <sup>nd</sup> Step	3 <sup>rd</sup> step
Cellulose: Starch (Ratio)	Glycerin% (w/w)	Citric acid% (w/w)
10:0		
9:1		
8:2		
7:3		
6:4	10	10
	20	20
5:5	30	30
4:6	40	40
3:7	50	50
2:8		
1:9		

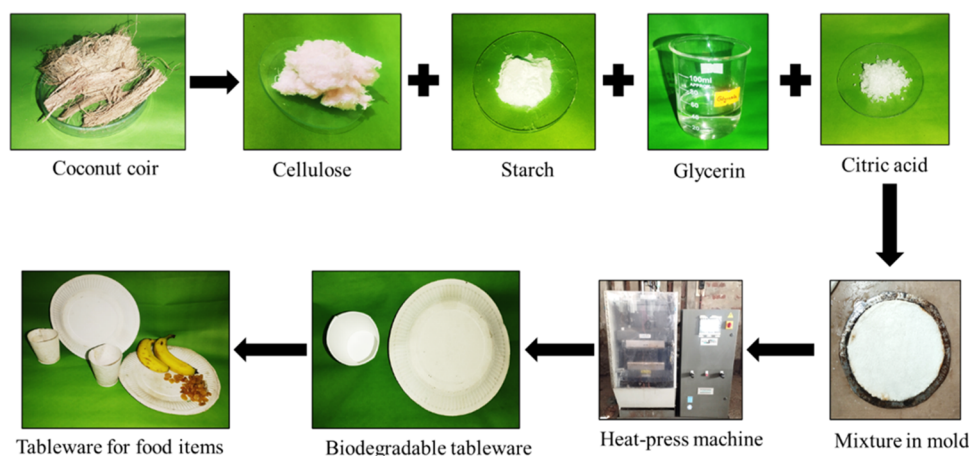


Figure 2. Schematic representation for the preparation of biodegradable tableware from coconut coir.

The schematic diagram for the preparation of biodegradable tableware is shown in Figure 2.

**2.4. Characterizations.** **2.4.1. FT-IR Spectroscopy.** FT-IR spectra were recorded using an attenuated total reflectance-Fourier transform infrared (ATR-FTIR) Shimadzu IRSpirit instrument (Japan) for the identification of functional groups. FT-IR spectra of the samples were recorded in the transmittance mode range of 4000–400  $\text{cm}^{-1}$  with an average of 32 scans.

**2.4.2. Scanning Electron Microscopy (SEM).** Scanning electron microscopy (SEM) images were observed to study the surface morphology. The specimens were gold-coated using a sputtering device (JEOL, JFC-1200) with carbon conductive tape (Ted Pella, Inc.) and visualized using ZEISS Sigma 300 VP (Germany) with an accelerating voltage of 15 kV.

**2.4.3. Thermogravimetric Analysis (TGA).** The thermal properties were investigated by a thermogravimetric analyzer (SHIMADZU TGA-50 Series, Japan). The amount of sample for each measurement was taken into consideration within 3–6 mg, placed in a platinum pan, and thermograms were recorded between 30 and 600  $^{\circ}\text{C}$  with a heating rate of 10  $^{\circ}\text{C}/\text{min}$  under a constant flow of nitrogen (2 mL/min).

**2.4.4. X-ray Diffraction (XRD).** Crystallographic investigation of samples was conducted using a Rigaku Smartlab SE,

Japan. X-ray generator tension and current were 40 kV and 30 mA, respectively. The wavelength of  $\text{Cu-K}\alpha$  was taken as 0.154 nm. A scan speed of 0.5 $^{\circ}/\text{min}$  and a step size of 0.02 $^{\circ}(2\theta)$  were used to acquire the data throughout the  $2\theta$  range of 4–60 $^{\circ}$ . The crystallinity was determined based on the ratio of the crystalline region's area to the total area in the XRD spectra. The crystallinity index and average crystallite size were calculated using eqs 4 and 5<sup>35</sup>

$$\begin{aligned} \text{crystallinity index, CI (\%)} \\ = \frac{\sum \text{area of crystalline peaks}}{\sum \text{area of crystalline and amorphous peaks}} \times 100\% \end{aligned} \quad (4)$$

$$\text{average crystallite size, } D = \frac{K\lambda}{\beta \cos \theta} \quad (5)$$

where  $K$  is the Scherrer constant (0.94);  $\lambda$  is the wavelength of  $\text{Cu K}\alpha$  radiation;  $\beta$  is the full width at half-maximum (fwhm) in radian, and  $\theta$  is the diffraction angle.

**2.4.5. Mechanical Tests.** Mechanical properties such as tensile strength (TS) and elongation at break (Eb %) of the tableware were measured by a Universal Testing Machine (Zwick Roell Z010, Japan) following the standard test method recommended by the American Society of Testing and Materials (ASTM D882).<sup>36</sup> At least five samples were tested

for each specimen, and each test was continued until tensile failure (maximum force capacity of 10 kN).

**2.4.6. Water Absorption Test.** The water absorption properties of tableware were determined according to ASTM D570 guidelines.<sup>35</sup> Water uptake percentage (%) was calculated using eq 6.

$$\text{water absorption (\%)} = \frac{W_m - W_d}{W_d} \times 100\% \quad (6)$$

where  $W_m$  is the weight of the sample as a function of time and  $W_d$  is the dry weight.

**2.4.7. Water Vapor Transmission Test.** Water vapor test was conducted by a textest AG, FX3180 CupMaster, ZURICH (Switzerland), and the test method was ASTM E96 with slight modification. Water vapor test method parameters were weighting interval: 0.50 h, test criterion: equilibrium, conditioning time: 1 h, test principle: wet cup, solvent: water, relative humidity (RH): 80%, velocity: 0.3 m/s, maximum deviation: 15%, test area: 50 cm<sup>2</sup>. The water vapor transmission rate (WVTR) was calculated according to eq 7.

$$\text{WVTR} = \frac{\Delta W}{\Delta t \cdot A} \quad (7)$$

where  $\Delta w/\Delta t$  (g/s) is the flux measured as weight loss of the cell per unit of time and  $A$  (m<sup>2</sup>) represents the actual exposed area.

**2.4.8. Water Contact Angle.** The static water contact angle was determined using the sessile drop method on a Kruss G-1 contact angle goniometer (Germany) at an ambient temperature. The test method was ASTM D5946 where a strip of the polymer test material was placed on a goniometer testing platform. Water droplets (3  $\mu$ L) were dispensed onto the surface using a syringe assembly (30 gauge needle), and images were recorded every 3 s.

**2.4.9. Soil Burial Test.** The biodegradability was tested using the soil burial method. The degree of biodegradation was monitored for a period of 1 month (30 days). The samples were cut into 4 cm  $\times$  4 cm pieces and buried under 0.15–0.40 m of soil.<sup>37</sup> The pH of the soil was neutral, and the moisture content of the soil was appraised as 40%. The percentage of degradation was measured after 7, 14, 21, and 30 days, respectively. Each sample was retrieved, cleaned, and dried at room temperature before measuring its weight. The degree of soil degradation (DSD) was calculated by using eq 8.

$$\text{degradation in soil (\%)} = \frac{(W_o - W_d)}{W_o} \times 100\% \quad (8)$$

where  $W_o$  and  $W_d$  are the initial and final dry weights (before and after degradation), respectively.

**2.4.10. Statistical Analysis.** All experiments were conducted three times in parallel, and the results were expressed in terms of mean  $\pm$  standard deviation. All of the data were analyzed using SPSS software version 16 (SPSS, Chicago, IL), where all data were statistically appropriate with no significant difference within the obtained values. Analysis of variance (ANOVA) was performed and the significance of each mean property value was determined ( $p < 0.05$ ).

### 3. RESULTS AND DISCUSSION

**3.1. Chemical Compositions of Coconut Coir.** Chemical composition refers to the presence of basic components in

a material. When it comes to fiber, it refers to the various components like ash, moisture, cellulose, hemicellulose, lignin, etc.<sup>38</sup> The chemical composition of coconut coir is given in Table 3. The percentage of moisture content of coir in this

**Table 3. Chemical Compositions of Coconut Coir**

components	amount (%)
moisture	12.40 $\pm$ 0.71
ash	2.10 $\pm$ 0.03
cellulose	38.17 $\pm$ 0.84

study was found by 12.40%. This result was close to the findings of Ewansiha et al. where the moisture content was calculated as 10.10%.<sup>27</sup> In this study, the ash content of coconut coir was found to be 2.10%, whereas Verma et al. reported that the ash content of coconut fiber was appraised as 2.22% which is almost similar to the present study.<sup>28</sup> Ash content was found to be 2.28% in coconut coir, as reported by Ewansiha et al.<sup>27</sup> Cellulose and lignin are the major components in coconut coir, and in this research, the cellulose content in coir was found to be 38.17  $\pm$  0.84% on a dry weight basis. In research, Geethamma et al. reported that the percentage of cellulose varied between 35 and 43%, whereas Kongkaew et al. reported that 33–41% of cellulose was present in coconut coir which was in line with our present study.<sup>39,40</sup> Moreover, Rosa et al. also found a similar percentage of cellulose (approximately 37%) and Das et al. found 43.44% of cellulose in their reports.<sup>41,42</sup> Recently, Kongkaew has reported 41–45% of lignin and 0.24–4.0% of hemicellulose content present in coir fiber.<sup>40</sup>

**3.2. Alkali Treatment of Coconut Coir.** Coir fiber was treated with 5, 10, 15, and 20% alkali solution, and after bleaching and drying, it was examined by ATR-FTIR, as shown in Figure 3. Previous research had shown that the carbonyl

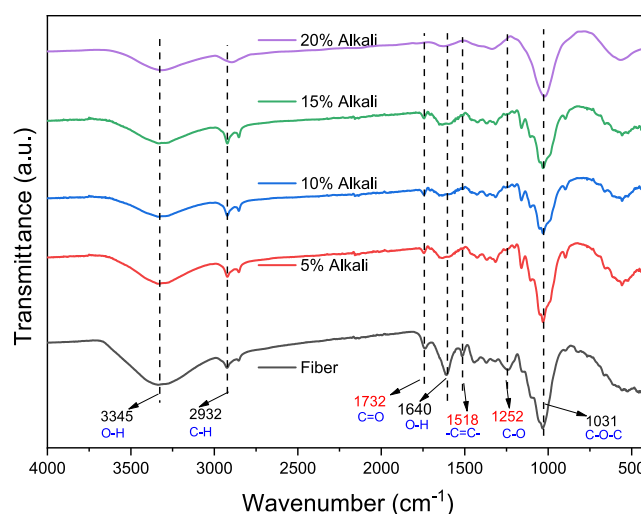


**Figure 3.** FT-IR spectra of coconut coir at different alkali treatments.

(C=O) unconjugated stretching vibration of ester and carbonyl group of hemicellulose in coir fibers were responsible for the significant peak at 1740 cm<sup>-1</sup>.<sup>43</sup> In this study, the peak at 1732 cm<sup>-1</sup> of coir fiber disappeared from FT-IR spectra after treating with 20% alkali, suggesting the removal of most hemicellulose and pectin. It also suggested treating with 5, 10, and 15% alkali was not enough to remove hemicellulose.

However, the characteristic peak at 1520–1510  $\text{cm}^{-1}$  was attributed to the stretch vibration of  $-\text{C}=\text{C}-$  in aromatic rings of lignin.<sup>44</sup> The significant response at 1300–1200  $\text{cm}^{-1}$  was induced by out-of-plane stretching of C–O in the aryl group of lignin and hemicellulose.<sup>43</sup> The notable peaks at 1518 and 1252  $\text{cm}^{-1}$  did not appear in the spectrum for cellulose as compared to native coir fibers, confirming the elimination of lignin from coir fiber.

In addition, cellulose treated with different alkali solutions showed similar absorption peaks at 3400, 2900, 1430, 1370, and 890  $\text{cm}^{-1}$ . The peak at 2900  $\text{cm}^{-1}$  was attributed to stretching vibrations of C–H, and remarkable responses between 3300 and 3500  $\text{cm}^{-1}$  ratified the presence of the O–H group. Moreover, peaks at 1430 and 1370  $\text{cm}^{-1}$  were assigned because of the bending vibration of C–O–H. Apart from this, the band at 896  $\text{cm}^{-1}$  was associated with the stretching vibration of C–O–C in the  $\beta$  (1  $\rightarrow$  4) glycosidic linkage of cellulose.<sup>45</sup> In the same way, notable bands at 1022, 1313, and 1374  $\text{cm}^{-1}$  were correlated to the bending movement of the C–O–C group in pyranose ring skeletal; vibration of C–C and C–O skeletal; and stretching movement of H-bonded O–H group in cellulose, respectively.<sup>46,47</sup>

**3.3. FT-IR Analysis to Confirm Cross-Linking.** FT-IR spectroscopy analysis is regarded as a valuable tool for the identification of key functional groups and bonding in a compound. Figure 4 illustrates the FT-IR results of the CA

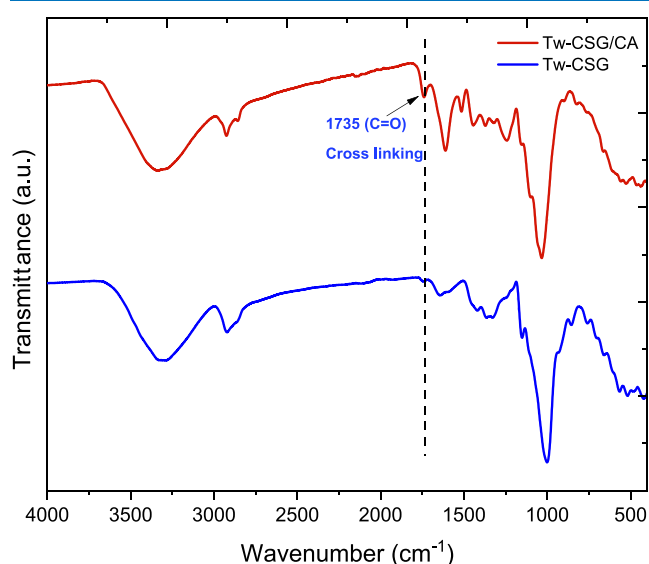


**Figure 4.** Indication of cross-linking in Tw-CSG/CA by FT-IR spectra (CA 10%).

content (10%) in tableware (Tw). In comparison to cellulose, starch, and glycerin-based tableware (Tw-CSG), tableware with CA (Tw-CSG/CA) exhibited a new band at 1735  $\text{cm}^{-1}$ , which might be due to stretching vibrations of carbonyl groups (C=O), suggesting the existence of carboxylic acid, ketones, or aldehydes compounds formed by the insertion of cross-linking agent.<sup>48</sup> CA, possessing three carboxylic groups, suggests that esterification happened between CA, glycerol, and ester linkage occurred between starch and cellulose. The inter- and intramolecular hydrogen bonds might be disrupted by the combination of CA with cellulose and starch chains through esterification.<sup>49</sup> By introducing hydrophobic ester

groups to substitute hydroxyl groups of starch, its hydrophilic character can be reduced.<sup>50</sup>

**3.4. Mechanical Properties.** In this research, cellulose as a main raw material, starch as a binder, and glycerol as a plasticizer made the material more flexible. In this polymeric material, CA was utilized as a cross-linking agent in between hydroxyl (OH) clusters in polymer molecules that significantly enhanced density, possessing improved mechanical properties.<sup>51</sup> On the contrary, higher content of CA substantially reduced the tensile strength, while improving elongation at break.<sup>52,53</sup> TS and percentage of Eb of cellulose-based tableware at various ratios of cellulose, starch, glycerin, and CA are graphically demonstrated in Figure 5.

Tw made from cellulose/starch (CS) blend composites were considered at different ratios from 10:0 to 1:9 for the investigation of mechanical properties. The TS value of the prepared biopolymer ranged from 4.2 to 15.6 MPa, and the percentage of Eb was varied from 0.62 to 1.42%. At the same time, the CS blend showed significant differences in TS with the increase of starch concentrations up to 6:4 ratio, and then the value was decreased. The CS ratio at 6:4 had the highest TS value of  $15.6 \pm 0.93$  MPa with the percentage of Eb of  $1.31 \pm 0.21\%$ , which might be due to the interfacial interaction between cellulose and starch.<sup>54</sup> Therefore, this ratio was taken into consideration for further investigation. Glycerol, a plasticizer, can make the biopolymer more flexible since the intermolecular bonds between the polymer chains are reduced that influences the mechanical properties.<sup>56</sup> In this study, glycerol was added to the optimized CS ratio at 6:4 with different ratios of the solute weight, ranging from 10 to 50% (w/w). Cellulose/starch/glycerol (CSG) blend biopolymer had TS ranging from 2.6 to 9.1 MPa, and the percentage of Eb ranged from 2.3 to 4.3%. However, the change in elongation was not proportionally related to glycerol content. It was noticed that the elongation of Tw increased as the concentration of glycerol increased for a certain percentage, then the value decreased. The highest percentage of elongation was found as  $4.3 \pm 0.18\%$ , with the addition of 20% glycerol to the CS composite. A higher elongation indicated the ensuring of more flexibility that can withstand deformation without fracturing easily. Furthermore, TS decreased after the addition of glycerol content in comparison to nonplasticized CS at the ratio of 6:4 blend because glycerol could act as a plasticizer that increased elongation but considerably decreased the tensile strength supported by several studies.<sup>48,55–57</sup>

Finally, CA as a cross-linker was added to the optimized CSG at the ratio (6:4–20%). CA was added at different ratios of solutes weight, ranging from 10 to 50% (w/w). The cellulose/starch/glycerol/citric acid (CSG/CA) biopolymer had TS ranging from 10.4 to 18.6 MPa and Eb% of 3.5 to 4.6%. The addition of 10% (w/w) CA into Tw-CSG improved TS compared to glycerol, and the TS value was observed as  $18.6 \pm 0.93$  MPa with a percentage of EB having  $3.5 \pm 0.16\%$ . Niu et al. prepared Tw from bagasse pulp fiber and starch using poly(dimethylsiloxane) (PDMS) coating to improve hydrophobicity, possessing a TS value of 21.2 MPa and the results were nearly similar to the present study. However, PDMS has several drawbacks, such as high cost, long process time, and modified process in different applications.<sup>58</sup> Moreover, it becomes soft and loses its structural integrity at elevated temperatures.<sup>59</sup> However, CA is a common organic acid found in fruits that is easily obtainable, nontoxic, and inexpensive.<sup>26</sup> In this research, CA was used as a cross-linking agent, which

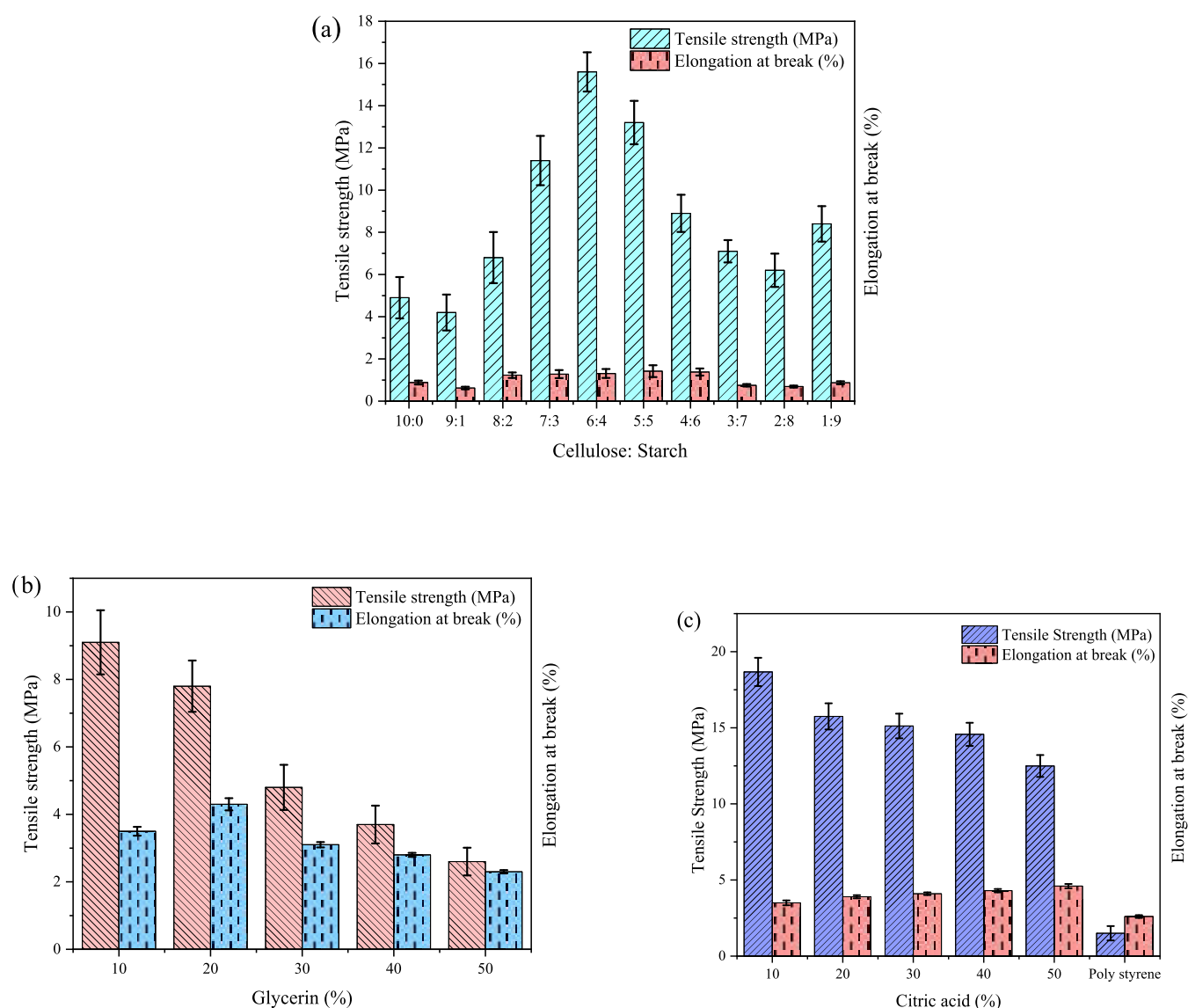


**Figure 5.** (a) TS and Eb% of cellulose: starch biocomposite, (b) TS and Eb% for tableware at different glycerol contents, and (c) TS and Eb% for tableware at different CA contents.

enhanced the mechanical strength as well as water resistance property of the polymeric material. There could be a synergistic impact, intermolecular interactions between the polymer matrix, and similar polysaccharide structures that lead to the rise of mechanical strength due to the addition of CA.<sup>60</sup> However, higher CA content can decrease tensile strength, since CA can act as both a cross-linker and plasticizer, as reported by Jiugao et al.<sup>61</sup> Cellulose and starch polymers can form ester linkages and hydrogen bonds with the hydroxyl and carboxyl groups of CA that might lead to the formation of a robust structure. As a result, the mechanical characteristics are concurrently enhanced and can resist the diffusion of water molecules.<sup>62</sup> Therefore, the optimized ratio of cellulose:starch in Tw was considered at 6:4, 20% of glycerin, and 10% of CA. The amount of glycerol and CA to be added should be decided based on TS and elongation required for a particular application. Mechanical properties of commercial PS-based Styrofoam (one time plate) were also investigated by UTM machine, and the results revealed that TS and percentage of Eb were noted as  $1.5 \pm 0.23$  MPa and  $2.6 \pm 0.17\%$ , respectively.

The results were quite lower than those of the optimized Tw prepared in this research.

### 3.5. Scanning Electron Microscopy (SEM) Analysis.

External morphology (texture) and orientation of materials in the samples were investigated by scanning electron microscopy (SEM). Figure 6a shows an SEM image of coir fiber which provided a detailed, magnified, and microstructure view of the fiber. Coir fibers seemed fibrous and had string-like appearance with irregular and rough surface. Cellulose fibers had a comparatively smooth surface at the microscale due to the elimination of hemicellulose and lignin after alkali treatment and the bleaching process shown in Figure 6b.

From a morphological point of view, a good adhesion between the components had presupposed a compact structure, in which starch was evenly distributed with cellulose, as illustrated in Figure 6c. The cellulose fibers were intertwined with starch, creating a network-like structure. In the SEM image, starch granules were identified as discrete spherical or oval structures of varying sizes. Glycerin is a liquid compound and hence could not be visible in SEM image, but could

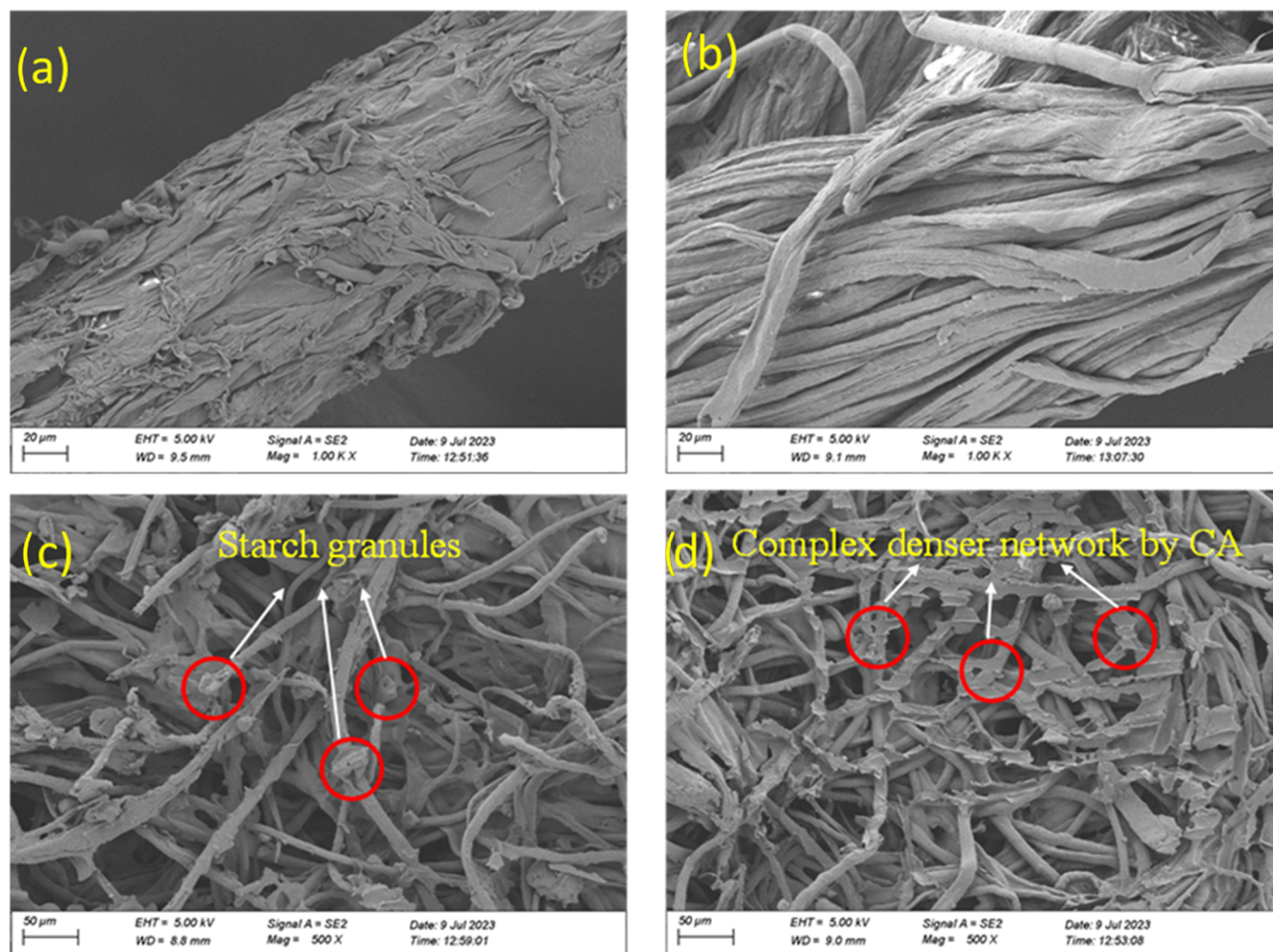


**Figure 6.** SEM image (a) coconut coir (scale 20  $\mu\text{m}$ , Mag: 1000 $\times$ ); (b) cellulose (scale 20  $\mu\text{m}$ , Mag: 1000 $\times$ ); (c) Tw-CSG (scale 50  $\mu\text{m}$ , Mag: 500 $\times$ ); (d) Tw-CSG/CA (scale 50  $\mu\text{m}$ , Mag: 500 $\times$ ).

contribute to the overall structure and cohesiveness of the blend. In Figure 6d, Tw-CSG/CA showed that cellulose fibers provided a structural framework with starch granules and CA particles dispersed throughout the complex matrix. The presence of cross-linking facilitated by CA leads to the formation of a denser network structure. Actually, cross-linking had modified the size and aggregation of cellulose as well as starch granules. SEM image revealed the mesh-like pattern, indicating improved cohesion by changing surface roughness.

**3.6. X-ray Diffraction (XRD) Analysis.** Powder XRD analysis was conducted to evaluate the crystallinity index of coir fibers, cellulose, Tw-CSG, and Tw-CSG/CA. The results are presented in Figure 7, and XRD patterns of cellulose exhibited characteristic diffraction peaks at  $2\theta = 14.6^\circ$  ( $1\bar{1}0$ ),  $16.5^\circ$  (110),  $22.6^\circ$  (200), and  $34.7^\circ$  (004) that was supported by previous study and confirmed the crystal lattice type I of native cellulose.<sup>63,64</sup> The gradually increasing intensity of cellulose peaks at  $2\theta = 16.5$  and  $22.6^\circ$  showed that the crystallinity of the material increased by chemical treatment. The crystallinity index (CI) and average crystallite size were calculated using eqs 4 and 5, respectively. The CI value increased significantly when transforming from coir fiber (43.27%) to cellulose (69.66%). The results were close to research conducted by Nang An et al., who found a CI value of 45.4% for coconut husk fiber and 72.7% for pure cellulose.<sup>65</sup>

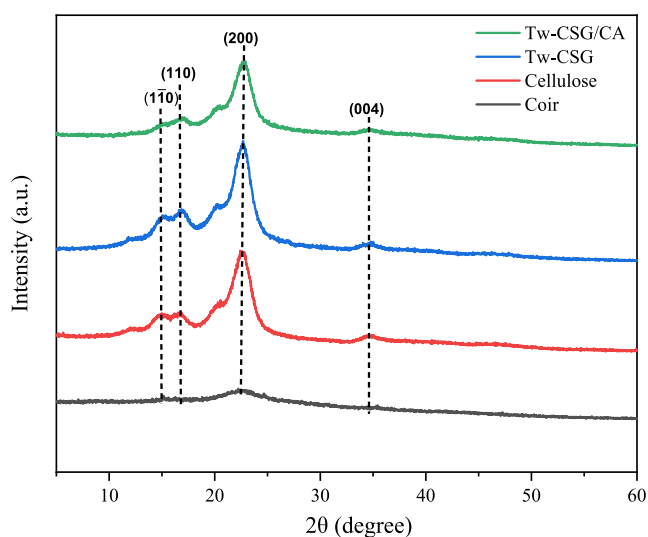


**Figure 7.** XRD patterns of coconut coir, cellulose, Tw-CSG, and Tw-CSG/CA.

The result of increasing the CI value indicated the elimination of hemicellulose and lignin. Actually, the CI value is affected by different sources of cellulose, chemical agents, and processing method.<sup>65</sup> In addition, the average crystallite size of untreated



coir was calculated as 6.50 nm, and the average crystallite size of cellulose was found as 2.73 nm.

It was noticed that identical characteristic peaks at  $2\theta = 16.5$  and  $22.6$  and  $34.7^\circ$  appeared in the two samples of tableware but with a small difference in the intensity of Tw-CSG/CA. It showed a much lower crystallinity index (45.51%) than Tw-CSG (56.28%) because CA might have disrupted inter- and intramolecular hydrogen bonding causing the amorphous polymer structure. Moreover, this change in crystallinity was attributed to the disruption of well-organized native cellulose microstructures, followed by the development of more amorphous cellulose structures of tableware. The presence of amorphous cellulose was highly advantageous for flexibility and elongation.<sup>35</sup> The addition of glycerol in Tw-CSG caused a decrease in CI due to increased amorphous regions and reduced ordering in the structure. After the addition of CA in Tw-CSG/CA, the CI value was further reduced due to its role in breaking down the cellulose structure. Sommer et al. reported that the degree of crystallinity decreased with increasing plasticizer and cross-linker concentration due to the reduction of interactions between matrix chains.<sup>66</sup>

**3.7. Thermogravimetric Analysis (TGA).** Thermogravimetric analysis was carried out to evaluate the thermal stability of Tw-CSG and Tw-CSG/CA through various stages of decomposition. It has been reported that the addition of fiber to starch has improved thermal stability because of enhanced adhesion between the fiber and the matrix, which reduces the loss of mass in the sample.<sup>67,68</sup> Figure 8 shows the TG curve of

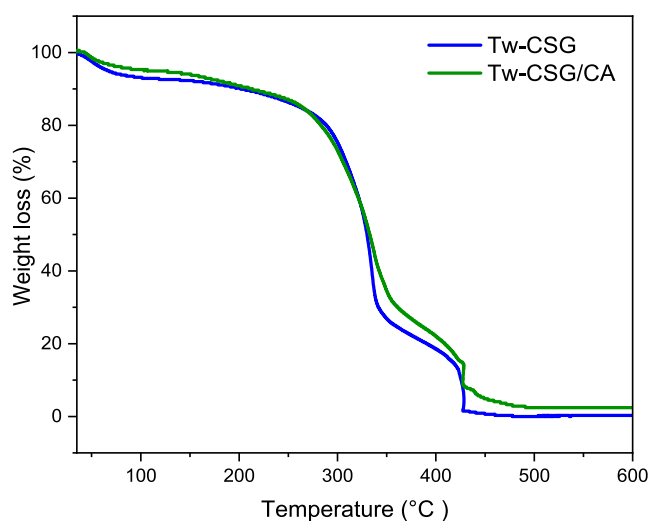


**Figure 8.** Comparison of TGA curves of tableware (Tw-CSG and Tw-CSG/CA).

Tw with the effect of cross-linking. The initial weight loss of 7–8% in both the samples was found in the range of 80–110 °C, bolstering the evaporation of moisture or bound water from the Tw sample. However, the first predominant stage of degradation in Tw-CSG started at 223 °C and terminated at 368 °C with a loss of 76.76% due to pyrolysis of thermoplastic starch and cellulose (Table 4). The weight loss in the second stage reached 99.07% in the temperature range of 395–442 °C corresponding to the breakdown of polymer backbone and degradation of polysaccharide structure (organic fragments) of the biopolymer.<sup>69</sup>

Figure 8 also illustrates that Tw cross-linked with CA (Tw-CSG/CA) showed significant thermal stability. The first

**Table 4.** Effect of Temperature on the Decomposition of Tw

composition	1st decomposition region		2nd decomposition region	
	temp. (°C)	wt. loss (%)	temp. (°C)	wt. loss (%)
Tw-CSG	223–368	76.76	395–442	99.07
Tw-CSG/CA	238–381	74.89	402–456	95.27

predominant stage of degradation was noticed between 238 and 381 °C with a percentage of weight loss of 74.89% due to the degradation of the polymer chain,<sup>70,71</sup> followed by further weight loss in the second degradation region around 402–456 °C (wt. loss 95.27%), corresponding to the breakdown of polymer backbone and degradation of polysaccharide structure (organic fragments) of the biopolymer.<sup>69</sup> Tw-CSG/CA exposed comparatively higher onset temperature and lower mass loss than Tw-CSG that might be explained in terms of binding of cellulose and glycerol to starch in the presence of CA. The improvement in thermal stability confirmed the addition of CA, and the adhesion between cellulose, glycerol, and starch in the synthesized biopolymer was enhanced.<sup>61</sup> Basically, CA decreases intra- and intermolecular interactions between cellulose–cellulose and starch–starch chains and strengthens the bonding interactions between the hydroxyl groups of cellulose and starch.<sup>72</sup>

**3.8. Water Absorption.** Native starch and cellulose are hydrophilic in nature and are cross-linked by CA that expect the reducing of water absorption rate. In the present study, the absorption of water for Tw-CSG and Tw-CSG/CA was compared to a period of time from 0 to 120 min. Figure 9

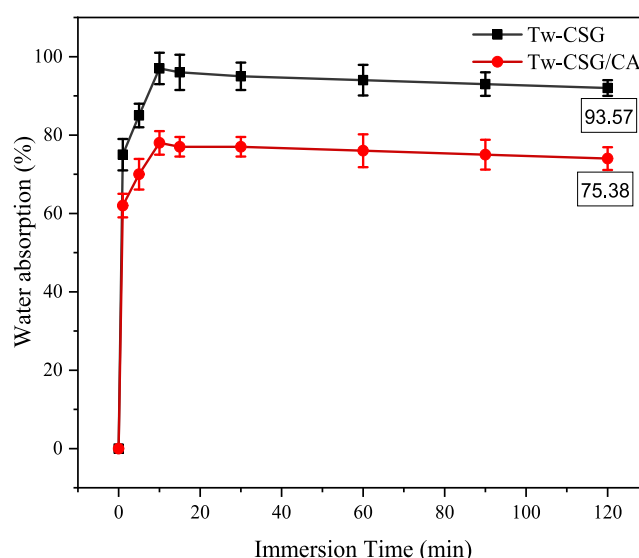


**Figure 9.** Water absorption performance of tableware (Tw-CSG, Tw-CSG/CA).

shows that all of the samples had a high absorption rate in the first 10 min of wetting time, and it was steady from 15 to 120 min, which was almost similar to previous work by Lee et al.<sup>73</sup> Moreover, Namphonsane et al. also performed water absorption test for 120 min and found that the water absorption decreased owing to increased amount of CA owing to network structure through cross-linking.<sup>74</sup> Gerezgiher et al. found similar results of water absorption (90–120% after 2 h) of films prepared from starch, glycerin, and CA.<sup>75</sup> Mahmud et al. also conducted a water absorption test for 120

min and claimed that high water absorption was attributed to the presence of hydrophilic starch and glycerol.<sup>76</sup> Steady increment of the amount of water absorbed as a function of time was expected until the process reached equilibrium condition.<sup>76</sup> High water absorption in Tw-CSG was attributed to the presence of glycerol and starch due to the hydrophilic character.<sup>77</sup> Samples prepared by adding CA slowed down the water absorption rate owing to the presence of CA that reduced the number of  $-OH$  groups by forming ester linkage between cellulose and starch, and lessened the hydrophilic character of the biopolymer.<sup>78</sup> Samples with CA retained their shapes with slight swelling and did not disintegrate into small pieces throughout the entire experiment, indicating good water resistivity. After 120 min, the rate of water absorption of Tw-CSG was calculated as  $93.57 \pm 2.11\%$ , whereas Tw-CSG/CA showed a percentage of  $75.38 \pm 0.85\%$ . This is evidence that the esterification reaction had reduced the number of free hydroxyl groups, causing the reduction of hydrophilicity. The reported results were quite similar to the findings of Heebthong et al. and Prachayawarakorn et al.<sup>79,80</sup> In fact, the chemical and physical bonding decreased the water absorption property.

**3.9. Water Vapor Transmission Rate (WVTR).** Water vapor transmission rate (WVTR) is the most studied property of packaging materials mainly because of the important role of water in spoilage reactions and preventing dehydration. Figure 10 indicates that the Tw-CSG blend polymer had a water

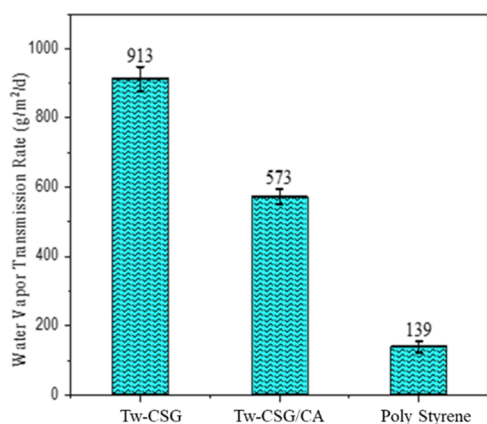


**Figure 10.** Comparison of water vapor transmission rates of tableware (Tw-CSG, Tw-CSG/CA) and polystyrene.

vapor transmission rate of  $913 \pm 12.05$  ( $\text{g}/\text{m}^2/\text{d}$ ). The value significantly reduced by  $573 \pm 8.03$  ( $\text{g}/\text{m}^2/\text{d}$ ) through the incorporation of CA. The addition of CA led to a significant decrease in WVTR, confirming the formation of a network structure. Food containers and Tw were often required to limit moisture transfer between the food and the surrounding atmosphere, WVTR should be as low as possible. Several authors also reported that the addition of CA in starch leads to a decrease in WVTR because the hydrophilic  $-OH$  groups were substituted by hydrophobic ester groups.<sup>48,60</sup> The lower WVTR indicated that oxygen and moisture could not easily penetrate the packaging material, which was more suitable for food preservation, and food could sustain for a long time without spoilage. In this research, the WVTR of commercial tableware (Styrofoam) made from polystyrene was also found to be  $139 \pm 4.57$  ( $\text{g}/\text{m}^2/\text{d}$ ).

**3.10. Water Contact Angle.** The water resistance performance of prepared Tw was evaluated by water contact angle (WCA) measurement to determine whether the prepared materials were hydrophobic or hydrophilic in nature. The value of the contact angle differed from  $0$  to  $180^\circ$ , where  $0^\circ$  indicated highly hydrophilic in nature and above  $90^\circ$  indicated hydrophobic in nature.<sup>36</sup> Though several researchers claimed that biomaterial surfaces with  $\text{WCA} > 65^\circ$  can be considered hydrophobic,<sup>81,82</sup> Figure 11 shows that the

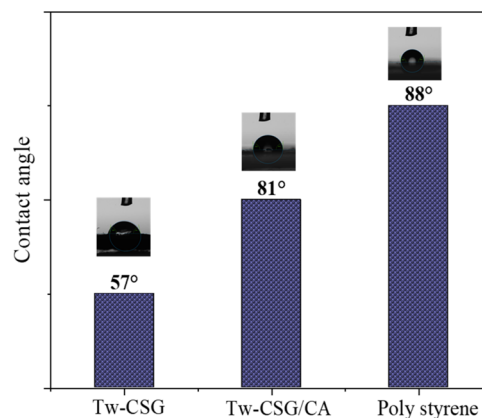


**Figure 11.** Water contact angle of tableware (Tw-CSG, Tw-CSG/CA) and polystyrene.

prepared biopolymer (Tw-CSG/CA) was less hydrophobic when compared to polystyrene-based Tw, which was almost hydrophobic. Tw without CA (Tw-CSG) had a contact angle of  $57^\circ$ . When CA was introduced, a cross-link formed, the surface became relatively rough, and contact angle increased to  $81^\circ$ . Tw prepared from bagasse pulp fiber and starch using poly(dimethylsiloxane) (PDMS) coating had a contact angle of  $121^\circ$ , as reported by Niu et al.<sup>83</sup> However, PDMS can absorb small hydrophobic molecules like biomolecules and drugs from solution, and it can easily pick up contaminants from the environment.<sup>84</sup> However, CA is nontoxic, inexpensive, and it enhanced the water resistance and improved water contact angle by cross-linking. Therefore, it can be said that the prepared materials could be used in a variety of consumer products, such as food containers, tableware, biodegradable utensils, and food packaging.

**3.11. Soil Burial Test.** Soil burial test was conducted to check the biodegradability of the prepared Tw. The weight loss of samples indicated the biodegradation of Tw by microorganisms. Figure 12 shows the degradation of all of the biopolymer samples after 1 month of burial in the soil, indicating the materials were biodegradable. After 14 days, Tw-CSG showed a significant reduction in thickness and weight. They changed their tonality and exhibited pores, showing the beginning of degradation while with CA (Tw-CSG/CA) 21 days were necessary. After 7 days of incubation, weight reduction of Tw-CSG and Tw-CSG/CA was 6.10 and 4.39%, respectively. After 30 days, the percentage of weight loss continued to increase over time and reached up to 44.27% for Tw-CSG and 39.18% for Tw-CSG/CA. In soil, water diffuses into the polymer sample causing swelling and enhancing biodegradation due to increases in microbial growths. The incorporation of CA decreased moisture absorption which caused the reduction of microbial attacks in cross-linked samples. These results agreed with the study reported by Maiti

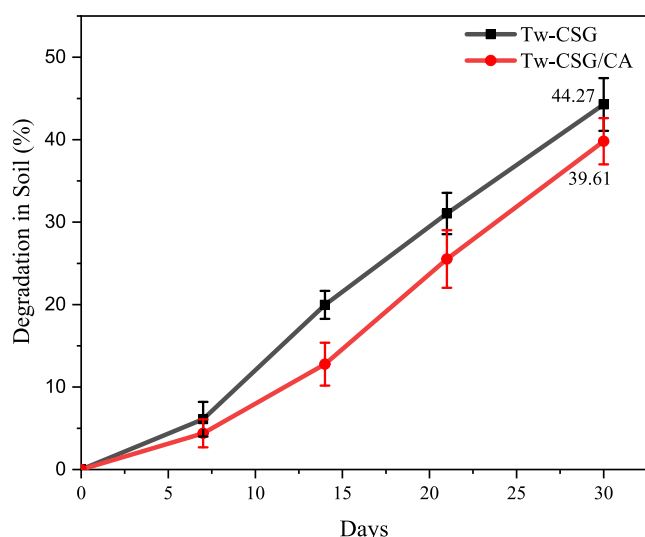


**Figure 12.** Comparison of the soil burial graph of tableware (Tw-CSG, Tw-CSG/CA).

and Ray et al., who observed that cross-linking slowed biodegradability in the first 15 days of soil burial test.<sup>85</sup> Tableware prepared from bagasse pulp and starch using poly(dimethylsiloxane) (PDMS) needed 100 days to degrade 74% of weight in soil, as reported by Niu et al.,<sup>83</sup> whereas, in this study, it was estimated that all of the samples prepared were biodegradable within 70–90 days (3 months). The formation of network structure by the use of CA was beneficial to many purposes that could slow down the degradation process.<sup>50</sup> Visual modifications of the samples were also seen after finishing the test. The samples were broken into pieces when touched, and micropores were observed, which increased the access sites for water and microorganisms and led to a higher percentage of biodegradation. Moreover, environmental factors such as temperature, moisture, pH, and biological activity could affect the rate of degradation.

#### 4. CONCLUSIONS

Coconut coir, a major byproduct, is renewable and recyclable for the preparation of environmentally friendly biodegradable utensils, such as plates, cups, boxes, and other catering products. In this study, cellulose was extracted from coir fiber, and with the addition of binder, plasticizer, and cross-linker, the durability of Tw was facilitated. The optimized ratio of cellulose to starch (w/w) was 6:4 with 20% glycerol and 10% CA. Tw with cross-linker showed excellent mechanical properties, thermal stability, contact angle, and water vapor transmission rate. Tw possessed TS of 18.6 MPa with 3.5% of Eb, whereas commercially available polystyrene had TS and percentage of Eb values of 1.5 MPa and 2.6%, respectively. Tw showed a lower contact angle ( $57^\circ$ ) in the absence of CA, but after incorporation of CA, the contact angle improved to  $81^\circ$ , while commercially available polystyrene possessed a contact angle of  $88^\circ$ . Moreover, the annexation of CA led to a significant decrease of water vapor transmission rate from 913 to 573 ( $\text{g}/\text{m}^2/\text{d}$ ), suggesting the formation of cross-linking. Apart from this, a notable percentage of weight loss was observed up to 39.18% (Tw-CSG/CA) after 30 days, indicating the biodegradable nature of Tw within 90 days. In addition, the thermal study results expressed the extended stability of Tw by  $238^\circ\text{C}$  due to the presence of network

structure after the addition of CA. Moreover, the fabricated Tw had promising qualities as a competitive alternative to Styrofoam-based plastic, including ease of manufacture, superior strength, and biodegradability. The highlighted routes will definitely contribute to a sustainable polymeric product to meet economic, environmental, and social needs.

#### ■ ASSOCIATED CONTENT

##### Supporting Information

The Supporting Information is available free of charge at <https://pubs.acs.org/doi/10.1021/acsomega.4c03031>.

Steps of cellulose extraction; fabrication of tableware; thermogravimetric analysis; and EDX mapping (PDF)

#### ■ AUTHOR INFORMATION

##### Corresponding Author

Mosummath Hosna Ara – Chemistry Discipline, Khulna University, Khulna 9208, Bangladesh;  
Phone: +8801711365072; Email: [hosnaara1@gmail.com](mailto:hosnaara1@gmail.com)

##### Authors

Md. Hafizul Islam – Chemistry Discipline, Khulna University, Khulna 9208, Bangladesh; Department of Chemistry, International University of Business Agriculture and Technology, Dhaka 1230, Bangladesh  
Mubarak A. Khan – Ministry of Textiles and Jute, Bangladesh Jute Mills Corporation, Dhaka 1000, Bangladesh  
Jannatul Naime – Chemistry Discipline, Khulna University, Khulna 9208, Bangladesh  
Md. Latifur Rahman – Bangladesh Jute Mills Corporation (BJMC), Dhaka 1000, Bangladesh  
Tania Akter Ruhane – Bangladesh Jute Mills Corporation (BJMC), Dhaka 1000, Bangladesh  
Md. Abu Rayhan Khan – Chemistry Discipline, Khulna University, Khulna 9208, Bangladesh; [orcid.org/0000-0002-9719-1266](https://orcid.org/0000-0002-9719-1266)

Complete contact information is available at: <https://pubs.acs.org/doi/10.1021/acsomega.4c03031>

##### Author Contributions

This work was conducted by all authors.

##### Notes

The authors declare no competing financial interest.

#### ■ ACKNOWLEDGMENTS

The authors are very grateful to Chemistry Discipline, Khulna University, and Sonali Bag Laboratory, Bangladesh Jute Mills Corporation, for laboratory and instrumental support.

#### ■ REFERENCES

- (1) Opara, U. L. A review on the role of packaging in securing food system: Adding value to food products and reducing losses and waste. *Afr. J. Agric. Res.* **2013**, *8* (22), 2621–2630.
- (2) Jan, B.; Rizvi, Q. U.; Shams, R. et al. Containers for Food Packaging Application. In *Micro-and Nano-Containers for Smart Applications*; Springer, 2022; pp 105–125.
- (3) Hidalgo-Crespo, J.; Moreira, C.; Jervis, F.; et al. Circular economy of expanded polystyrene container production: Environmental benefits of household waste recycling considering renewable energies. *Energy Rep.* **2022**, *8*, 306–311.
- (4) Zhao, N.; Zhu, J.; Zhao, M.; et al. Twenty bisphenol analogues in take-out polystyrene-made food containers: Concentration levels,

- stimulated migration, and risk evaluation. *Environ. Sci. Pollut. Res.* **2023**, *30* (4), 10516–10526.
- (5) Dey, S.; Veerendra, G. T. N.; Babu, P. S. S. A.; et al. Degradation of plastics waste and its effects on biological ecosystems: A scientific analysis and comprehensive review. *Biomed. Mater. Devices* **2024**, *2* (1), 70–112.
- (6) Dalei, G.; Das, S. K.; Mohapatra, S. S.; et al. In situ crosslinked Schiff base biohydrogels containing Carica papaya peel extract: application in the packaging of fresh berries. *Sustainable Food Technol.* **2023**, *1* (6), 906–920.
- (7) Garrison, T. F.; Murawski, A.; Quirino, R. L. Bio-based polymers with potential for biodegradability. *Polymers* **2016**, *8* (7), No. 262.
- (8) Jahangiri, F.; Mohanty, A. K.; Misra, M. Sustainable biodegradable coatings for food packaging: challenges and opportunities. *Green Chem.* **2024**, *26*, 4934–4974, DOI: 10.1039/D3GC02647G.
- (9) Armir, N. A. Z.; Zulkifli, A.; Gunaseelan, S.; et al. Regenerated cellulose products for agricultural and their potential: A review. *Polymers* **2021**, *13* (20), No. 3586.
- (10) Habibi, Y.; Lucia, L. A.; Rojas, O. J. Cellulose nanocrystals: chemistry, self-assembly, and applications. *Chem. Rev.* **2010**, *110* (6), 3479–3500.
- (11) Geng, H.; Yuan, Z.; Fan, Q.; et al. Characterisation of cellulose films regenerated from acetone/water coagulants. *Carbohydr. Polym.* **2014**, *102*, 438–444.
- (12) Sirviö, J. A.; Liimatainen, H.; Niinimäki, J.; et al. Sustainable packaging materials based on wood cellulose. *RSC Adv.* **2013**, *3* (37), 16590–16596.
- (13) Miao, C.; Hamad, W. Y. Cellulose reinforced polymer composites and nanocomposites: a critical review. *Cellulose* **2013**, *20*, 2221–2262.
- (14) Abbood, I. S.; Odaa, S. A.; Hasan, K. F.; et al. Properties evaluation of fiber reinforced polymers and their constituent materials used in structures—A review. *Mater. Today: Proc.* **2021**, *43*, 1003–1008.
- (15) Stanislas, T. T.; Mahamat, A. A.; Bilba, K.; et al. Dimensional stability, durability and performance of hybrid recycled cellulose fibres reinforcing earth-based materials. *J. Compos. Mater.* **2023**, *57* (22), 3463–3478.
- (16) Mamani, D. C.; Nole, K. S. O.; Montoya, E. E. C.; et al. Minimizing organic waste generated by pineapple crown: a simple process to obtain cellulose for the preparation of recyclable containers. *Recycling* **2020**, *5* (4), No. 24.
- (17) Gunarathne, D. S.; Udugama, I. A.; Jayawardena, S.; et al. Resource recovery from bio-based production processes in developing Asia. *Sustainable Prod. Consumption* **2019**, *17*, 196–214.
- (18) Saha, K. K.; Hossain, M.; Ali, M.; et al. Feasibility study of coconut coir dust briquette. *J. Bangladesh Agric. Univ.* **2016**, *12* (2), 369–376.
- (19) Oladele, I. O.; Adelani, S. O.; Makinde-Isola, B. A. et al. Coconut/Coir Fibers, their Composites and Applications. In *Plant Fibers, their Composites, and Applications*; Elsevier, 2022; pp 181–208.
- (20) Hasan, K. M. F.; Horváth, P. G.; Kóczán, Z.; et al. Thermo-mechanical properties of pretreated coir fiber and fibrous chips reinforced multilayered composites. *Sci. Rep.* **2021**, *11*, No. 3618.
- (21) Siakeng, R.; Jawaid, M.; Asim, M.; et al. Alkali treated coir/pineapple leaf fibres reinforced PLA hybrid composites: Evaluation of mechanical, morphological, thermal and physical properties. *eXPRESS Polym. Lett.* **2020**, *14* (8), 717–730.
- (22) Coupland, J. N.; Shaw, N. B.; Monahan, F. J.; et al. Modeling the effect of glycerol on the moisture sorption behavior of whey protein edible films. *J. Food Eng.* **2000**, *43* (1), 25–30.
- (23) Guilbert, S.; Gontard, N.; Cuq, B. Technology and applications of edible protective films. *Packag. Technol. Sci.* **1995**, *8* (6), 339–346.
- (24) Bruna, A. S. M.; de Oliveira Reis João, H.; Lindaiá, S. C.; et al. Characterization of cassava starch films plasticized with glycerol and strengthened with nanocellulose from green coconut fibers. *Afr. J. Biotechnol.* **2017**, *16* (28), 1567–1578.
- (25) Carr, S.; Szalodobagyi, E. Citric or Acetic Acid Effects on the Crosslinking of PVOH, 2022.
- (26) Krumova, M.; López, D.; Benavente, R.; et al. Effect of crosslinking on the mechanical and thermal properties of poly (vinyl alcohol). *Polymer* **2000**, *41* (26), 9265–9272.
- (27) Ewansiha, C.; Ebhoaye, J. E.; Asia, I. O.; et al. Proximate and mineral composition of coconut (*Cocos nucifera*) shell. *Int. J. Pure Appl. Sci. Technol.* **2012**, *13* (1), 57–60.
- (28) Verma, D.; Gope, P. C.; Shandilya, A.; et al. Coir fibre reinforcement and application in polymer composites. *J. Mater. Environ. Sci.* **2013**, *4* (2), 263–276.
- (29) Cifriadi, A.; Panji, T.; Wibowo, N. A.; et al. Bioplastic production from cellulose of oil palm empty fruit bunch. *IOP Conf. Ser.: Earth Environ. Sci.* **2017**, *62*, No. 012011, DOI: 10.1088/1755-1315/65/1/012011.
- (30) Prado, K. S.; Spinacé, M. A. Isolation and characterization of cellulose nanocrystals from pineapple crown waste and their potential uses. *Int. J. Biol. Macromol.* **2019**, *122*, 410–416.
- (31) Sipiao, B.; Paiva, R.; Goulart, S.; et al. Effect of chemical modification on mechanical behaviour of polypropylene reinforced pineapple crown fibers composites. *Procedia Eng.* **2011**, *10*, 2028–2033.
- (32) Hassani, F.-Z. S. A.; Salim, M. H.; Kassab, Z.; et al. Crosslinked starch-coated cellulosic papers as alternative food-packaging materials. *RSC Adv.* **2022**, *12* (14), 8536–8546.
- (33) Cerqueira, J. C.; da Silva Penha, J.; Oliveira, R. S.; et al. Production of biodegradable starch nanocomposites using cellulose nanocrystals extracted from coconut fibers. *Polimeros* **2017**, *27*, 320–329.
- (34) de Andrade, M. R.; Nery, T. B. R.; de Santana e Santana, T. I.; et al. Effect of cellulose nanocrystals from different lignocellulosic residues to chitosan/glycerol films. *Polymers* **2019**, *11* (4), No. 658.
- (35) Rumi, S. S.; Liyanage, S.; Abidi, N. Conversion of low-quality cotton to bioplastics. *Cellulose* **2021**, *28*, 2021–2038.
- (36) Marichelvam, M. K.; Jawaid, M.; Asim, M. Corn and rice starch-based bio-plastics as alternative packaging materials. *Fibers* **2019**, *7* (4), No. 32.
- (37) Wang, H.; Wei, D.; Zheng, A.; et al. Soil burial biodegradation of antimicrobial biodegradable PBAT films. *Polym. Degrad. Stab.* **2015**, *116*, 14–22.
- (38) Thangaraj, P. Proximate Composition Analysis. In *Pharmacological Assays of Plant-Based Natural Products*; Springer, 2016; Vol. 71, pp 21–31.
- (39) Geethamma, V.; Mathew, K. T.; Lakshminarayanan, R.; et al. Composite of short coir fibres and natural rubber: effect of chemical modification, loading and orientation of fibre. *Polymer* **1998**, *39* (6–7), 1483–1491.
- (40) Kongkaew, P. In *Mechanical Properties of Banana and Coconut Fibers Reinforced Epoxy Polymer Matrix Composites*; Proceedings of Academics World 17th International Conference, Tokyo, Japan, 2016.
- (41) Rosa, M.; Medeiros, E.; Malmonge, J.; et al. Cellulose nanowhiskers from coconut husk fibers: Effect of preparation conditions on their thermal and morphological behavior. *Carbohydr. Polym.* **2010**, *81* (1), 83–92.
- (42) Das, D.; Kaundinya, D.; Sarkar, R.; et al. Shear strength improvement of sandy soil using coconut fibre. *Int. J. Civ. Eng. Technol.* **2016**, *7* (3), 297–305.
- (43) Yongvanich, N. Isolation of nanocellulose from pomelo fruit fibers by chemical treatments. *J. Nat. Fibers* **2015**, *12* (4), 323–331.
- (44) Elanthikkal, S.; Gopalakrishnanpanicker, U.; Varghese, S.; et al. Cellulose microfibrils produced from banana plant wastes: Isolation and characterization. *Carbohydr. Polym.* **2010**, *80* (3), 852–859.
- (45) Ibrahim, M. M.; El-Zawawy, W. K.; Jüttke, Y.; et al. Cellulose and microcrystalline cellulose from rice straw and banana plant waste: preparation and characterization. *Cellulose* **2013**, *20*, 2403–2416.
- (46) Liu, C.-F.; Ren, J. L.; Xu, F.; et al. Isolation and characterization of cellulose obtained from ultrasonic irradiated sugarcane bagasse. *J. Agric. Food Chem.* **2006**, *54* (16), 5742–5748.

- (47) Gao, X.; Chen, K. L.; Zhang, H.; et al. Isolation and characterization of cellulose obtained from bagasse pith by oxygen-containing agents. *BioResources* **2014**, *9* (3), 4094–4107.
- (48) Reddy, N.; Yang, Y. Citric acid cross-linking of starch films. *Food Chem.* **2010**, *118* (3), 702–711.
- (49) Zuraida, A.; Yusliza, Y.; Anuar, H.; et al. The effect of water and citric acid on sago starch bio-plastics. *Int. Food Res. J.* **2012**, *19* (2), 715–719.
- (50) Seligra, P. G.; Jaramillo, C. M.; Famá, L.; et al. Biodegradable and non-retrogradable eco-films based on starch–glycerol with citric acid as crosslinking agent. *Carbohydr. Polym.* **2016**, *138*, 66–74.
- (51) Woggum, T.; Sirivongpaisal, P.; Wittaya, T. Properties and characteristics of dual-modified rice starch based biodegradable films. *Int. J. Biol. Macromol.* **2014**, *67*, 490–502.
- (52) Qin, Y.; Wang, W.; Zhang, H.; et al. Effects of citric acid on structures and properties of thermoplastic hydroxypropyl amylo maize starch films. *Materials* **2019**, *12* (9), No. 1565.
- (53) Sharmin, N.; Sone, I.; Walsh, J. L.; et al. Effect of citric acid and plasma activated water on the functional properties of sodium alginate for potential food packaging applications. *Food Packag. Shelf Life* **2021**, *29*, No. 100733.
- (54) Gulati, K.; Lal, S.; Arora, S. Synthesis and characterization of PVA/Starch/CMC composite films reinforced with walnut (*Juglans regia* L.) shell flour. *SN Appl. Sci.* **2019**, *1*, No. 1416.
- (55) Zuraida, A.; Yusliza, Y.; Anuar, H.; et al. The effect of water and citric acid on sago starch bio-plastics. *Int. Food Res. J.* **2012**, *19* (2), 715–719.
- (56) Tarique, J.; Sapuan, S.; Khalina, A. Effect of glycerol plasticizer loading on the physical, mechanical, thermal, and barrier properties of arrowroot (*Maranta arundinacea*) starch biopolymers. *Sci. Rep.* **2021**, *11* (1), No. 13900.
- (57) Gao, C.; Pollet, E.; Avérous, L. Properties of glycerol-plasticized alginate films obtained by thermo-mechanical mixing. *Food Hydrocolloids* **2017**, *63*, 414–420.
- (58) Lin, L.; Chung, C.-K. PDMS microfabrication and design for microfluidics and sustainable energy application. *Micromachines* **2021**, *12* (11), No. 1350.
- (59) Müller, A.; Wapler, M. C.; Wallrabe, U. A quick and accurate method to determine the Poisson's ratio and the coefficient of thermal expansion of PDMS. *Soft Matter* **2019**, *15* (4), 779–784.
- (60) Ghanbarzadeh, B.; Almasi, H.; Entezami, A. A. Improving the barrier and mechanical properties of corn starch-based edible films: Effect of citric acid and carboxymethyl cellulose. *Ind. Crops Prod.* **2011**, *33* (1), 229–235.
- (61) Jiugao, Y.; Ning, W.; Xiaofei, M. The effects of citric acid on the properties of thermoplastic starch plasticized by glycerol. *Starch-Stärke* **2005**, *57* (10), 494–504.
- (62) Ghanbarzadeh, B.; Almasi, H.; Entezami, A. A. Physical properties of edible modified starch/carboxymethyl cellulose films. *Innovative Food Sci. Emerging Technol.* **2010**, *11* (4), 697–702.
- (63) Gong, J.; Li, J.; Xu, J.; et al. Research on cellulose nanocrystals produced from cellulose sources with various polymorphs. *RSC Adv.* **2017**, *7* (53), 33486–33493.
- (64) Sankhla, S.; Sardar, H. H.; Neogi, S. Greener extraction of highly crystalline and thermally stable cellulose micro-fibers from sugarcane bagasse for cellulose nano-fibrils preparation. *Carbohydr. Polym.* **2021**, *251*, No. 117030.
- (65) Nang An, V.; Nhan, H. T. C.; Tap, T. D.; et al. Extraction of high crystalline nanocellulose from biorenewable sources of Vietnamese agricultural wastes. *J. Polym. Environ.* **2020**, *28*, 1465–1474.
- (66) Sommer, A.; Staroszczyk, H.; Sinkiewicz, I.; et al. Preparation and characterization of films based on disintegrated bacterial cellulose and montmorillonite. *J. Polym. Environ.* **2021**, *29*, 1526–1541.
- (67) Ma, X.; Yu, J.; Kennedy, J. F. Studies on the properties of natural fibers-reinforced thermoplastic starch composites. *Carbohydr. Polym.* **2005**, *62* (1), 19–24.
- (68) Thawien, W. Characteristics and properties of rice starch films reinforced with palm pressed fibers. *Int. Food Res. J.* **2010**, *17*, 535–547.
- (69) Zhou, X.-Y.; Jia, D. M.; Cui, Y. F.; et al. Kinetics analysis of thermal degradation reaction of PVA and PVA/starch blends. *J. Reinf. Plast. Compos.* **2009**, *28* (22), 2771–2780.
- (70) Holland, B. J.; Hay, J. N. Thermal degradation of nylon polymers. *Polym. Int.* **2000**, *49* (9), 943–948.
- (71) Alvarez, V. A.; Vázquez, A. Thermal degradation of cellulose derivatives/starch blends and sisal fibre biocomposites. *Polym. Degrad. Stab.* **2004**, *84* (1), 13–21.
- (72) Shi, R.; Zhang, Z.; Liu, Q.; et al. Characterization of citric acid/glycerol co-plasticized thermoplastic starch prepared by melt blending. *Carbohydr. Polym.* **2007**, *69* (4), 748–755.
- (73) Lee, H.; You, J.; Jin, H. J.; et al. Chemical and physical reinforcement behavior of dialdehyde nanocellulose in PVA composite film: A comparison of nanofiber and nanocrystal. *Carbohydr. Polym.* **2020**, *232*, No. 115771.
- (74) Namphonsane, A.; Suwannachat, P.; Chia, C. H.; et al. Toward a circular bioeconomy: Exploring pineapple stem starch film as a plastic substitute in single use applications. *Membranes* **2023**, *13* (5), No. 458.
- (75) Gerezgihier, A.; Szabó, T. Crosslinking of starch using citric acid. *J. Phys.: Conf. Ser.* **2022**, *2315*, No. 012036, DOI: 10.1088/1742-6596/2315/1/012036.
- (76) Muhammad, A.; Rashidi, A. R.; Buddin, M. Effect of coconut fiber reinforcement on mechanical properties of corn starch bioplastics. *Int. J. Eng. Technol.* **2018**, *7* (4.18), 267–270.
- (77) Judawisastira, H.; Sitohang, R.; Marta, L. In *Water Absorption and Its Effect on the Tensile Properties of Tapioca Starch/Polyvinyl Alcohol Bioplastics*, IOP Conference Series: Materials Science and Engineering; IOP Publishing, 2017.
- (78) Cioica, N.; Fecete, R.; Chelcea, R.; et al. Water absorption and degradation of packages based on native corn starch with plasticizers. *Stud. Univ. Babeş-Bolyai, Chem.* **2015**, *60* (1), 45–55.
- (79) Heebthong, K.; Ruttarattanamongkol, K. Physicochemical properties of cross-linked cassava starch prepared using a pilot-scale reactive twin-screw extrusion process (REX). *Starch-Stärke* **2016**, *68* (5–6), 528–540.
- (80) Prachayawarakorn, J.; Tamseekhram, J. Chemical modification of biodegradable cassava starch films by natural mono-, di- and tricarboxylic acids. *Songklanakarin J. Sci. Technol.* **2019**, *41* (2), 355–362.
- (81) Vogler, E. A. Structure and reactivity of water at biomaterial surfaces. *Adv. Colloid Interface Sci.* **1998**, *74* (1–3), 69–117.
- (82) Yue, H.; Zheng, Y.; Zheng, P.; et al. On the improvement of properties of Bioplastic composites derived from wasted cottonseed protein by rational cross-linking and natural fiber reinforcement. *Green Chem.* **2020**, *22* (24), 8642–8655.
- (83) Niu, S.; Chang, Q.; He, W.; et al. Mechanically strong, hydrostable, and biodegradable starch–cellulose composite materials for tableware. *Starch-Stärke* **2022**, *74* (7–8), No. 2200019.
- (84) Van Meer, B.; de Vries, H.; Firth, K.; et al. Small molecule absorption by PDMS in the context of drug response bioassays. *Biochem. Biophys. Res. Commun.* **2017**, *482* (2), 323–328.
- (85) Maiti, S.; Ray, D.; Mitra, D. Role of crosslinker on the biodegradation behavior of starch/polyvinylalcohol blend films. *J. Polym. Environ.* **2012**, *20*, 749–759.